

Improved surface morphology and mobility of AlGa_N/Ga_N HEMT grown on silicon substrate

Xueliang Zhu, Jun Ma, Tongde Huang, Ming Li, Ka Ming Wong, Kei May Lau*

Department of Electronic and Computer Engineering, Hong Kong University of Science and Technology, Clear Water Bay, Kowloon, Hong Kong

Received 11 July 2011, revised 18 August 2011, accepted 23 August 2011
Published online 2 December 2011

Keywords Ga_N HEMT, MOCVD, reverse leakage current

* Corresponding author: e-mail EEKMLAU@UST.HK, Phone: +852 23587049, Fax: +852 23581485

High mobility AlGa_N/Ga_N HEMT was grown on silicon substrates by MOCVD. Smooth and crack-free wafers were obtained by implementation of an AlN/AlGa_N super-lattice interlayer. We also found that the carrier gases have a great influence on the surface morphology of the AlGa_N barrier. With a proper ratio of carrier gases, the

AlGa_N surface is significantly improved. With other optimized growth conditions, the electron mobility of HEMT can be as high as 1650 cm²/Vs. HEMT devices are also fabricated and the reverse biased gate leakage current was reduced to 6.5 μA/mm at V_{gs} = -35 V.

© 2011 WILEY-VCH Verlag GmbH & Co. KGaA, Weinheim

1 Introduction

AlGa_N/Ga_N high electron mobility transistors (HEMTs) on silicon (Si) are promising power devices due to the low cost, and availability of large diameter Si substrates compared with sapphire and silicon carbide. However, the large lattice and thermal mismatch between III-nitride and Si results in cracks and defects in the epitaxial layer. Many methods have been utilized to solve these difficulties, such as low-temperature AlN inter-layers [1], multiple AlGa_N transition layer [2] as well as AlN/AlGa_N stacked inter-layer [3]. These inter-layers or transition layers can provide compressive stress on the Ga_N and compensate thermal mismatch induced tensile stress. As a result, the cracks density is greatly reduced or crack-free material can be achieved.

Much work has been devoted to improve the performance of HEMTs grown on Si to widen its applications. Many techniques developed in the past for HEMTs on sapphire and SiC may be applied to HEMT growth on silicon too. In the HEMT structure, the AlGa_N barrier is one of the critical layers. It has been shown that the AlGa_N surface morphology has a great influence on both the electron mobility [4] and gate leakage current of device [5] on sapphire. For the normal AlGa_N layer with Al composition around 30%, researchers had found that the ammonia flow, or V/III ratio, influences the surface morphology greatly

[4]. Higher ammonia flow usually results in rougher AlGa_N surfaces. There are also line-shaped defects on the AlGa_N surface and these defects can induce high reverse gate leakage current in device [5].

For HEMT structures grown on silicon, the surface defects and their influence on devices have been studied in detail [6, 7], however, little attention was paid to the growth parameters which influence surface morphology. In this work, we have investigated the growth conditions that influence the surface morphology of AlGa_N from both macroscopic and microscopic scales. We used an AlN/Ga_N super-lattice interlayer to compensate thermal mismatch induced tensile stress. Crack-free Ga_N film with smooth surface was obtained. We also found that the carrier gases have great influence on the surface morphology of AlGa_N. After optimization the carrier gas ratio between N₂ and H₂, a smooth, line-shaped-defects free surface was realized. A high Hall mobility was measured in this HEMT structure and the reverse gate leakage was reduced in the fabricated devices.

2 Experimental

The AlGa_N/Ga_N HEMT structure was grown on 2-inch Si substrates in an AIXTRON2000HT MOCVD system. Trimethylgallium (TMGa), trimethylaluminum (TMAI), trimethylindium (TMIIn) and ammonia (NH₃) were used as

the Ga, Al, In and N precursors, respectively. Biscyclopentadienyl magnesium (Cp_2Mg) and silane (SiH_4) were used as the p- and n-type doping sources. Prior to growth, the substrates were heated up to 1140 °C for 10 min under a H_2 ambience to remove the native oxide on the surfaces. Then a 40 nm AlN nucleation layer was grown, followed by a SiN partial mask. After growth of 800 nm undoped GaN on the SiN mask, eight periods of AlN(6nm)/ $Al_{0.19}Ga_{0.81}N$ (26nm) or AlN(6nm)/GaN(28nm) superlattice interlayer with a total thickness of 300nm was grown at 1130 °C to prevent the formation of cracks. Subsequently, a continuous 1 μm GaN buffer layer was grown at 1160 °C on the interlayer with the first 125 nm doped with magnesium. Finally 20 nm $Al_{0.3}Ga_{0.7}N$ modulated-doped barrier layer was grown on top of the continuous 1 μm GaN buffer layer. The whole structure of AlGaN/GaN HEMT on Si (111) substrate is shown in Fig. 1. During the growth of the AlGaN barrier layer, a mixture of H_2 and N_2 was used as carrier gases. Three samples were grown with different interlayer or H_2/N_2 ratio. The detail information is given in Table 1.

After growth, Normarski interference optical microscopy and atomic force microscopy (AFM) were used to investigate the surface morphology from both macroscopic and microscopic scales. The two dimensional electron gas (2DEG) density and mobility of the AlGaN/GaN sample were characterized at room temperature (RT) by van der Pauw Hall measurements. HEMT devices were also fabricated using materials with different surface morphology. Ti/Al/Ni/Au multi-layer metals were used as source and drain ohmic contacts. Ni/Au was used as gate metal for Schottky contact.

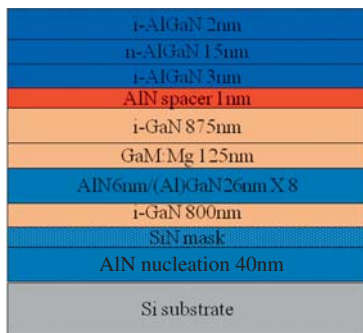


Figure 1 Structure of AlGaN/GaN HEMT on Si (111) substrate.

3 Results and discussion

The AlN/AlGaN interlayer can provide sufficient compressive stress so that the whole wafer is crack-free. However, the wafer surface is very rough both in macroscopic and microscopic scale, which can be seen in Figs. 2 and 3 for sample A. Moreover, there are also many line-shaped defects on the AFM image of sample A. During the growth of AlGaN in sample B, the ratio of N_2 in the carrier gas was increased from 7% to 33%. The surface morphology was greatly improved and the root-mean-square (RMS) roughness was reduced from 1 nm to 0.7 nm in a

5 $\mu m \times 5 \mu m$ scanned area. The line-shaped defects also disappeared. It is believed that the diffusion length of Al is longer in N_2 atmosphere, so the AlGaN surface becomes smoother. Yamaguchi also found that the AlGaN/GaN quantum wells grown on sapphire have better quality when they were grown in N_2 compared with H_2 [8].

Table 1 Summary of the HEMT structure, growth conditions.

Sample No.	Interlayer structure	N_2 % in AlGaN growth
A	AlN(6nm)/ $Al_{0.19}Ga_{0.81}N$ (26nm)	7%
B	AlN(6nm)/ $Al_{0.19}Ga_{0.81}N$ (26nm)	33%
C	AlN(6nm)/GaN(28nm)	33%

Table 2 Material characterization of samples A, B, and C.

Sample No.	RMS roughness on 5 $\mu m \times 5 \mu m$	Mobility ($cm^2/V s$)	Sheet carrier concentration ($10^{13} cm^{-2}$)
A	1 nm	1250	-1.97
B	0.7 nm	1460	-1.5
C	0.61 nm	1650	-1.53

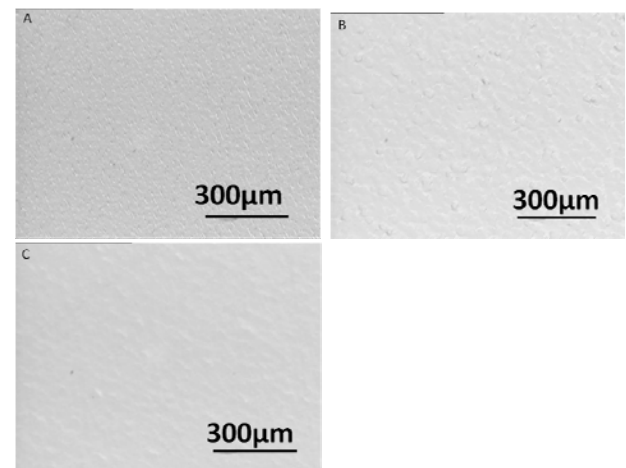


Figure 2 Surface morphology of sample A, B, and C under Nomarski interference optical microscopy,

Even though the surface appears to be very smooth in the microscopic scale, the samples with AlN(6nm)/ $Al_{0.19}Ga_{0.81}N$ (26nm) superlattice interlayer look very rough under Nomarski optical microscopy. Next the AlN(6nm)/ $Al_{0.19}Ga_{0.81}N$ (26nm) superlattice interlayer was replaced by a AlN(6nm)/GaN(28nm) layer in sample C. Compared with Al atoms, Ga atoms have longer diffusion length and smooth GaN can be grown on AlN in the interlayer. As a result, HEMT with this interlayer shows very smooth surface under Nomarski microscopy and the RMS roughness is further reduced to 0.61 nm in a 5 $\mu m \times 5 \mu m$ scanned area. The electron mobility was also greatly increased from 1250 cm^2/Vs to 1650 cm^2/Vs . To our knowledge, this is comparable to the best reported mobility result for HEMTs grown on Si [9].

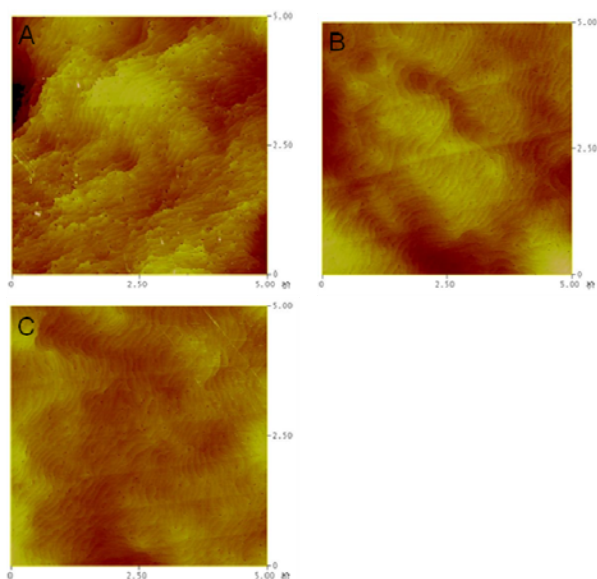


Figure 3 AFM images of sample A, B, and C. The scan area is $5\ \mu\text{m} \times 5\ \mu\text{m}$ and the vertical scale is 8 nm for all samples.

HEMT devices were also fabricated using sample A and sample C. The DC output and transfer characteristics with device dimensions of $L_g/W_g/L_{gs}/L_{gd} = 2/10/1/1\ \mu\text{m}$ were measured. Both of the devices have the same transconductance of 245 mS/mm. Both of the forward and reverse gate current of sample A and C are shown in Fig. 4. The reverse gate leakage current of sample C is much smaller in the whole measured range. At a gate bias of -35 V, the reverse gate leakage current is as low as $6.5\ \mu\text{A}/\text{mm}$ for the device fabricated on sample C, while it is $26\ \mu\text{A}/\text{mm}$ for the device fabricated on sample A, which may be due to the line-shaped defects on the AlGaIn surface. These defects were reported to cause large gate leakage current for AlGaIn/GaN HEMT grown on sapphire substrate [5]. Similar effects are observed here for HEMTs grown on Si.

Table 3 DC output and transfer characteristics of sample A and C.

Sample No.	G_m (mS/mm)	$I_{\text{dss}}@V_{\text{ds}} = 6\ \text{V}, V_{\text{gs}} = 2\ \text{V}$ (mA/mm)	$I_{\text{gs}}@V_{\text{gs}} = -35\ \text{V}$ ($\mu\text{A}/\text{mm}$)
A	245	846	26
C	245	943	6.5

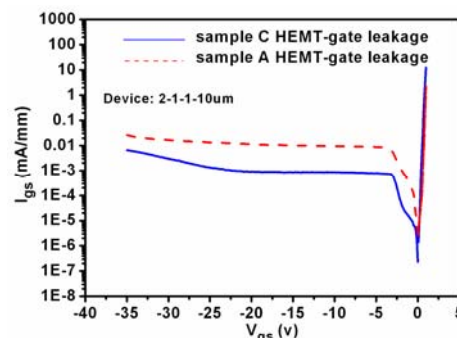


Figure 4 Forward and reverse gate current of sample A and C.

4 Conclusion

Through the combination of AlN/GaN super-lattice interlayer and proper N_2/H_2 ratio, the AlGaIn/GaN HEMT has a smooth surface and the electron mobility was also greatly increased from $1250\ \text{cm}^2/\text{Vs}$ to $1650\ \text{cm}^2/\text{Vs}$ moreover, the device shows a small reverse biased gate leakage current of $6.5\ \mu\text{A}/\text{mm}$.

Acknowledgements This work was supported in part by the grant ITS/523/09 from Hong Kong Special Administrative Government (HKSAR).

References

- [1] J. Blasing, A. Reiher, A. Dadgar, A. Diez, and A. Krost, *Appl. Phys. Lett.* **81**, 2722 (2002).
- [2] Kai Cheng, M. Leys, J. Derluyn, S. Degroote, D.P. Xiao, A. Lorenz, S. Boeykens, M. Germain, and G. Borghs, *J. Cryst. Growth* **298**, 822 (2007).
- [3] Wang Hui, Liang Hu, Wang Yong, Ng Kar-Wei, Deng Dong-Mei, and Lau Kei-May, *Chin. Phys. Lett.* **27**, 038103 (2010).
- [4] S. Keller, G. Parish, P. T. Fini, S. Heikman, C. H. Chen, N. Zhang, S. P. DenBaars, and U. K. Mishra, *J. Appl. Phys.* **86**, 5850 (1999).
- [5] Yugang Zhou, Rongming Chu, Jie Liu, Kevin J. Chen, and Kei May Lau, *Phys. Status Solidi C* **2**, 2663 (2005).
- [6] H. Sasaki, S. Kato, T. Matsuda, Y. Sato, M. Iwami, and S. Yosida, *Jpn. J. Appl. Phys.* **45**, 2531 (2006).
- [7] S. L. Selvaraj, T. Suzue, and T. Egawa, *Appl. Phys. Express* **2**, 111005 (2009).
- [8] S. Yamaguchi, M. Kariya, M. Kosaki, Y. Yukawa, H. Amano, and I. Akasaki, *Proc. Int. Workshop on Nitride Semiconductors, IPAP Conf. Ser.* **1**, pp. 141.
- [9] K. Cheng, M. Leys, S. Degroote, J. Derluyn, B. Sijmus, P. Favia, O. Richard, H. Bender, M. Germain, and G. Borghs, *Jpn. J. Appl. Phys.* **47**, 1553 (2008).